

# Measuring Anisotropic Thermal Conduction in Polyisobutylene Following Step Shear Strains

Hadjira Iddir, David C. Venerus, and Jay D. Schieber

Dept. of Chemical and Environmental Engineering and Center of Excellence in Polymer Science and Engineering,  
Illinois Institute of Technology, Chicago, IL 60616

*The connection between polymer chain orientation and several macroscopic properties in a polymer melt was studied using mechanical and optical techniques. Anisotropic thermal conductivity following shear deformation was measured using forced Rayleigh light scattering, the refractive index tensor is followed using birefringence measurements, and the stress was measured mechanically in a parallel-plate rheometer. The thermal diffusivity measured in the flow and neutral directions increased and decreased, respectively, immediately following the deformation. These quantities then relaxed to the equilibrium value on the time-scale of the stress-relaxation memory. Comparison of the difference between measured flow and neutral direction thermal diffusivities with the analogous flow-induced birefringence in the same deformation provided indirect evidence for a linear relation between stress and thermal diffusivity at two different values of strain. Mechanical measurements were used to characterize the memory of the fluid.*

## Introduction

Recent theoretical work has postulated the existence of anisotropic thermal conduction in polymeric liquids undergoing deformation. Most work has focused on dilute polymer solutions (Bird et al., 1997; Curtiss and Bird, 1996; Öttinger and Petrillo, 1996). However, the earliest work was applied by van den Brule to a polymer melt using a network theory (van den Brule, 1989; van den Brule and O'Brien, 1990). Öttinger (1998) also used a recently developed nonequilibrium thermodynamics formalism that includes relativistic effects to show that the thermal conductivity of a general viscous fluid undergoing shear can be anisotropic, with a quadratic dependence on shear rate.

These studies consider a generalization to Fourier's Law for which the thermal conductivity is described by a tensor, instead of a scalar

$$\mathbf{q} = -\mathbf{k} \cdot \nabla T, \quad (1)$$

where  $\mathbf{q}$  is the heat flux vector,  $T$  is temperature, and  $\mathbf{k}$  is the thermal conductivity tensor. The anisotropy in  $\mathbf{k}$  is caused by chain orientation induced by flow. Since the chain orientation is a function of the history of the imposed deformation,

the thermal conductivity tensor may be time dependent  $\mathbf{k}(t)$  for a prescribed flow history.

These works consider a shear flow whereby  $v_1 = \dot{\gamma}(t)x_2$ , and  $v_2 = v_3 = 0$ . It is well known (Bird et al., 1987) that such a shear flow induces anisotropy in the stress field for polymeric liquids

$$\boldsymbol{\tau} = \begin{bmatrix} \tau_{xx} & \tau_{yx} & 0 \\ \tau_{xy} & \tau_{yy} & 0 \\ 0 & 0 & \tau_{zz} \end{bmatrix}, \quad (2)$$

where  $\boldsymbol{\tau}$  is the extra stress tensor. It is also well established for polymer melts that an analogous anisotropy is induced in the refractive index tensor  $\mathbf{n}$ . More importantly, for flow fields that are not too strong, there exists a linear relationship between these two tensors (Fuller, 1995; Janeschitz-Kriegl, 1983)

$$\mathbf{n} - \frac{1}{3} \delta \text{tr}(\mathbf{n}) = C\boldsymbol{\tau}, \quad (3)$$

called the *stress-optic rule* and  $C$  is called the *stress-optic coefficient*. Existence of an analogous relationship between stress  $\boldsymbol{\tau}$  and thermal conductivity  $\mathbf{k}$ , or refractive index  $\mathbf{n}$  and thermal conductivity, has not yet been tested.

Correspondence concerning this article should be addressed to J. D. Schieber.

Experimental studies of heat conduction in *cross-linked* polymers have already revealed an anisotropic thermal conductivity under elongational stretch (Broerman et al., 1999; Tautz, 1959), however. These studies have revealed that thermal conductivity is enhanced along the direction of chain orientation.

On the other hand, measurements of thermal conductivity (or diffusivity) in flowing polymer liquids are somewhat scarce, and data that have been published are somewhat ambiguous. For example, in a sample of polydimethylsiloxane (PDMS), the thermal conductivity in the shear direction was shown to exhibit a maximum as a function of shear rate (Chitrangrad and Picot, 1981). A polyethylene sample, however, was seen to go through a minimum with shear rate in one study (Wallace et al., 1985), and a maximum in another (Picot et al., 1982). The reasons for the discrepancy are not clear, but may have to do with the relative invasiveness of the procedure.

In this article we present quantitative results, obtained using a noninvasive optical technique, demonstrating deformation-induced anisotropic conduction in a polymer melt and its subsequent relaxation. In particular, we examine the evidence for a stress-thermal rule.

### Forced Rayleigh Light Scattering Technique

We have used forced Rayleigh light scattering (FRLS) (Eichler et al., 1986) to measure thermal diffusivity in a polyisobutylene melt following a step shearing strain. The FRLS method has been used previously to study diffusive transport in a wide range of systems (Eichler et al., 1986) including measurements of thermal diffusion in polymer solutions (Köhler et al., 1995) and anisotropic thermal diffusivity in nematic liquid crystals (Rondelez et al., 1978; Veletskas et al., 1982). Details of our FRLS optical setup and the procedures used to measure thermal diffusivity in quiescent polymer liquids are given elsewhere (Venerus et al., 1999). The setup is shown in Figure 1.

Stated briefly, the technique uses crossed beams of a writing laser ( $\text{Ar}^+$ ) to induce a fringe pattern with period  $\Lambda$  in the sample, which contains dye that absorbs the impinging light. By rapid radiationless decay, the dye then creates a sinusoidal temperature field with modulation amplitude  $\delta T$ . As a consequence of the temperature dependence of the refractive index, the temperature field creates an optical (phase) grating in the sample.

Because the grating period  $\Lambda$  is much smaller than the spot size of the writing laser, the dynamics of the grating temperature field  $\delta T = T(x, t) - T_{\text{bulk}}(t)$  can be decoupled from the bulk temperature  $T_{\text{bulk}}$  in the sample. Furthermore, since the experiment satisfies conditions for the plane grating approximation (Eichler et al., 1986; Rondelez et al., 1978),  $\delta T$  is governed by

$$\rho \hat{C}_p \frac{\partial}{\partial t} \delta T = k_{ii} \frac{\partial^2}{\partial x_i^2} \delta T + KI(t) \cos(2\pi x_i/\Lambda) \quad (4)$$

where  $\rho$  is the polymer density,  $\hat{C}_p$  is the specific, constant-pressure heat capacity,  $k_{ii}$  is the  $ii$ -component of the thermal conductivity tensor,  $K$  is the absorptivity of the sample at the writing laser wavelength (515 nm), and  $I(t)$  is the time-dependent intensity of the writing laser.

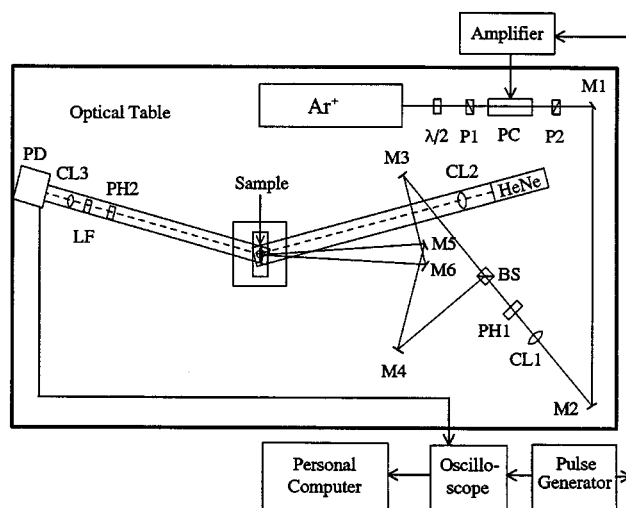


Figure 1. FRLS setup used in the study.

Component abbreviations:  $\text{Ar}^+$  = Argon ion writing laser; HeNe = Helium-Neon reading laser;  $\lambda/2$  = half-wave plate; P1, P2 = Glan prisms; PC = Pockels Cell used to chop the writing beam; M1-M6 = mirrors; CL1-CL3 = convex lenses for focusing; PH1, PH2 = pinholes to remove scattered light; BS = beamsplitter; LF = line filter that allows only HeNe to pass; PD = photodetector.

By reorienting the grating in the sample, different components of the thermal conductivity tensor can be probed. Equation 4 applies only when studying the flow ( $i=1$ ) and neutral ( $i=3$ ) directions, and contains no flow effects, since the temperature grating is created and decays only after the step strain is imposed. In Eq. 4 it is also assumed that the temperature dependence of  $k_{ii}$  can be neglected, which is justified since  $\delta T$  is typically of the order  $0.01^\circ\text{C}$ .

The writing laser is pulsed using a Pockels cell (PC) combined with Glan prisms (P1 and P2), which allow the laser to be switched on and off rapidly. Following a pulse from the writing laser, the grating temperature decays according to

$$\delta T \propto \exp^{-t/\tau_g}, \quad (5)$$

where the grating relaxation time is given by

$$\tau_g = \frac{\Lambda^2}{4\pi^2 D_{ii}}, \quad (6)$$

and where  $D_{ii} = k_{ii}/\rho \hat{C}_p$  is the thermal diffusivity in the  $i$ -direction. In arriving at Eq. 5, it has been assumed that the thermal diffusivity is constant during the time-scale of the grating decay  $\tau_g$ , which is typically of the order one ms. This assumption is plausible, because  $D_{ii}$  is expected to change on the time-scale of polymer chain relaxation ( $\approx 45$  s), which is several orders of magnitude larger than  $\tau_g$ .

These assumptions are confirmed *a posteriori*, during data analysis.

Dynamics of the grating were probed by a low-power reading laser (HeNe, 633 nm). When introduced at the Bragg angle, this beam is diffracted by the thermal grating with a diffraction efficiency proportional to  $(\delta T)^2$ . A photodetector

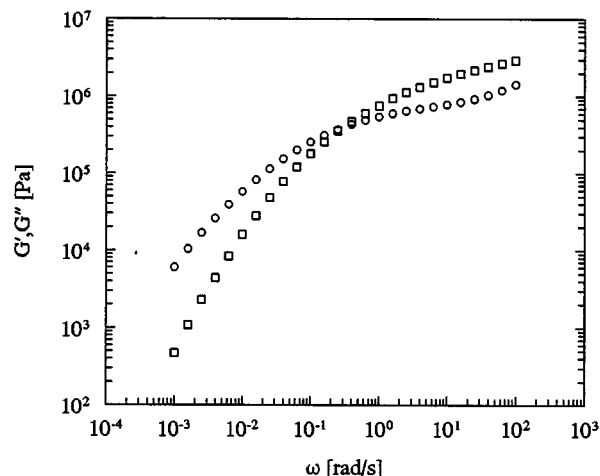


Figure 2. Storage and loss moduli measured using a Rheometrics (RMS-800) rheometer for the poly-isobutylene sample used in this study.

(PD) detects the first-order diffracted beam, which decays according to Eq. 5, along with coherently and incoherently scattered light producing a voltage that decays according to

$$V(t) = \bar{A}\exp(-2t/\tau_g) + \bar{B}\exp(-t/\tau_g) + \bar{C} \quad (7)$$

where  $\bar{A}$ ,  $\bar{B}$ , and  $\bar{C}$  are constants. Using an oscilloscope as a fast analog-to-digital converter, the signal is stored on a personal computer for analysis. The constant  $\bar{C}$  is measured at long times following the pulse, whereas  $\bar{A}$ ,  $\bar{B}$  and  $\tau_g$  were fit to the data by a Levenburg-Marquardt method described elsewhere (Press et al., 1992; Venerus et al., 1999). Several checks were performed on the curve-fitting procedure as shown below.

## Materials and Procedure

The poly-isobutylene sample had broad molecular weight distribution and a weight-average molecular weight of approximately 85,000. Small-amplitude oscillatory shear measurements were conducted at 25°C using torsional flow geometry in a Rheometrics Mechanical Spectrometer (RMS-800). These data are shown in Figure 2, and indicate that the viscosity is  $7.3 \times 10^6$  poise. The average relaxation time, as determined from a weighted average of the time constants found from a fit of discrete relaxation spectrum, is approximately 45 s.

A dye known as quinizarin, which absorbs light at a wavelength of 515 nm and is nearly transparent at 633 nm, was uniformly dispersed within the polymer. The concentration of the dye and pulse time of the writing laser were chosen such that the bulk temperature rise in the sample was less than 0.1°C. The writing laser was pulsed at a frequency of 20 Hz, meaning that 20 independent measurements of thermal diffusivity were taken every second. The equilibrium value of thermal diffusivity for this material measured using FRLS in the quiescent state was previously found to be  $D_{eq} = 6.56 \times 10^{-4}$  cm<sup>2</sup>/s with an uncertainty of roughly one percent (Venerus et al., 1999).

Step strain deformations were imposed on the polymer in a parallel-plate device. One plate was stationary, while the other was driven by several stiff springs, and released by interrupting current to an electromagnet that holds the mobile plate in a cocked position. Each plate had a glass window that formed an optical path through the sample after the step strain had been imposed. Shear strains equal to four and eight were used. The step strain is imposed in less than 75 ms, as determined from a simple optical experiment. From a shear-wave propagation analysis (Bird et al., 1987), we estimate the time required to reach vanishing fluid velocity to be on the order of one ms. Also, all experiments were conducted at room temperature, which was  $25 \pm 0.5^\circ\text{C}$ .

Birefringence experiments were performed using a simple optical arrangement in which the sample was positioned between crossed polarized (Janeschitz-Kriegl, 1983). The relative intensity  $I/I_0$  from such an arrangement is measured

$$\frac{I}{I_0} = \sin^2\left(\frac{\delta}{2}\right), \quad (8)$$

from which the retardance  $\delta$  can be found, where

$$\delta = \frac{\pi d \Delta n_{13}}{\lambda}. \quad (9)$$

Here,  $d$  is the thickness of the sample,  $\lambda$  is the wavelength of the laser impinging on the sample, and  $\Delta n_{13} = n_{11} - n_{33}$  is the sought-after birefringence. By following the intensity transmitted as a function of time, the relaxation in the birefringence may be found.

## Experimental Results and Conclusions

A sample waveform at a time of 150 ms following the step strain is shown in Figure 3, which plots the voltage from the photodetector both during and following the pulse of the writing laser. Only the voltage following the pulse is fit by Eq.

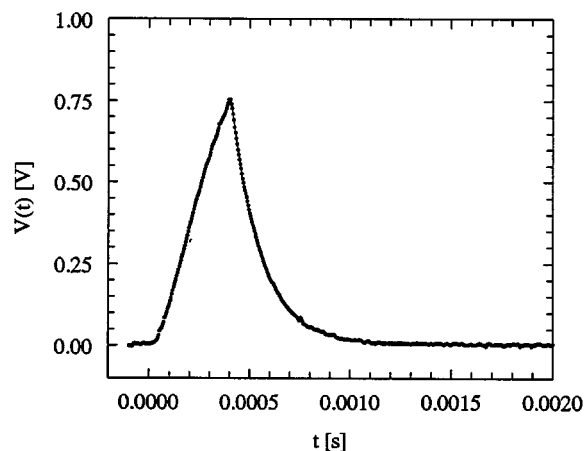


Figure 3. Photodetector voltage vs. time following a step strain of eight.

The origin of the time axis is 150 ms after the imposition of the strain. The symbols are the data and the solid line (decay only) is the fit of Eq. 7 giving a decay time  $\tau_g = 0.644$  ms.

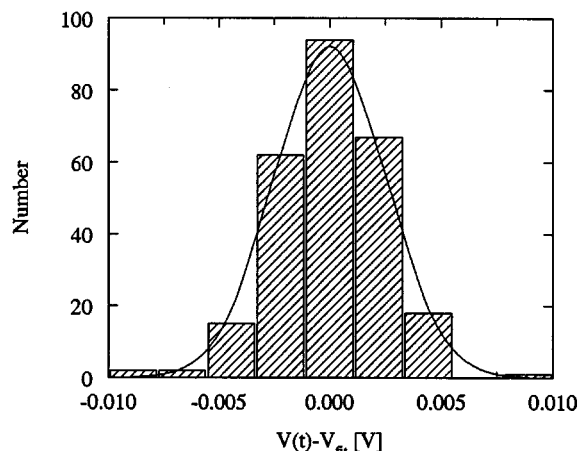


Figure 4. Histogram of the residuals  $V(t) - V_{\text{fit}}$  of the waveform shown in Figure 3.

The solid line is a Gaussian distribution with the same mean and variance as the residuals.

7. The solid line is a fit of this equation. However, it is mostly obscured by the data.

Figure 4 is a histogram of the residuals  $V(t) - V_{\text{fit}}$ . Figure 5 shows the fractional residuals  $[V(t) - V_{\text{fit}}]/V(t)$  as a function of time. The Gaussian distribution of the residuals, and the absence of a pattern in time confirm the validity of Eq. 7; they also verify our nonlinear curve-fitting procedure, and the assumption of constant thermal diffusivity during the decay of a grating.

Several voltage waveforms collected during the imposition of the deformation were analyzed but not used in this study. These waveforms, although similar in appearance to the one shown in Figure 3, could not be fit by the expression given in Eq. 7. This observation is not surprising since one would expect flow to smear the grating resulting in a larger grating decay rate than in the absence of flow. Bulk flow effects, if not properly accounted for, would cause an artifactual de-

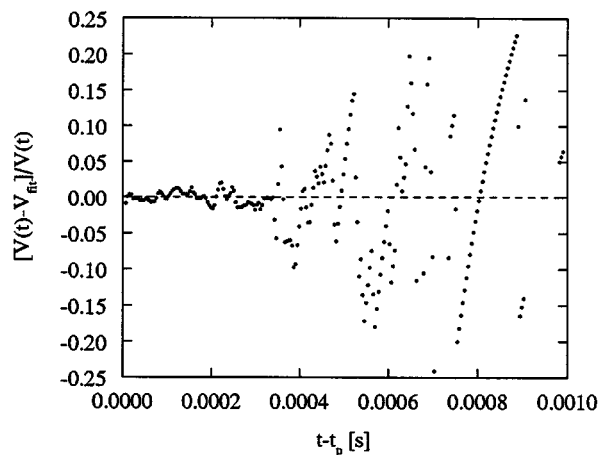


Figure 5. Fractional residuals of the waveform shown in Figure 3 as a function of time minus the pulse width  $t_p$ .

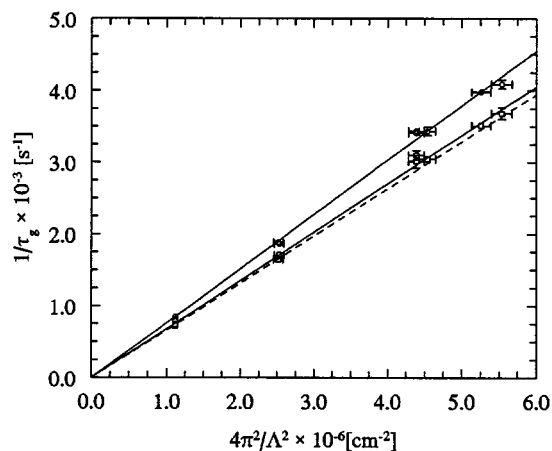


Figure 6. Dependence of grating relaxation time  $\tau_g$  on grating period  $\Lambda$  according to Eq. 6 for two values of time following a step strain of eight with the grating in the flow direction.

Solid lines through circles ( $\circ$ ) correspond to a time of 0.15 s and through the squares ( $\square$ ) correspond to a time of 1.5 s. The dashed line represents the result for a quiescent liquid found from an earlier study. Slopes of the lines give thermal diffusivity  $D_{11}$ .

crease in  $\tau_g$  and increase  $D_{11}$ . The generalization of Eq. 4 to include the effects of flow is not trivial, but would seem necessary unless the grating relaxation  $\tau_g$  is much smaller than the grating period  $\Lambda$  divided by the magnitude of the velocity. It appears that flow effects have not been properly taken into account in a previous study in which FRLS was used to measure thermal diffusivity in the constant-rate flow of a polymer melt through a slit (Miyamoto and Nagashima, 1996).

Validation of Eq. 4 can be confirmed by checking the dependence of the grating relaxation time with the grating period. According to Eq. 6, a plot of  $1/\tau_g$  vs.  $4\pi^2/\Lambda^2$  should be linear with a slope equal to the thermal diffusivity  $D_{11}$ . If  $D_{11}$  is a function of time (but constant during the decay of a grating) following the step strain, then isochronal values of  $\tau_g$  over a range of  $\Lambda$  must be used to make this check.

Figure 6 shows such a plot for several times following the imposition of a strain of 8 with the grating oriented in the flow direction. Each data point represents a result from a single waveform (of the kind shown in Figure 3) at a given time following the imposition of the strain. Each solid line was fit to points corresponding to a given time (but varying  $\Lambda$ ) following the step strain. The good correlation of the data points with the straight lines is consistent with the use of Eq. 4, and confirms the validity of Fourier's Law generalized to allow anisotropy. The slopes of the solid lines correspond to thermal diffusivity measured in the flow direction  $D_{11}$ , at different times. From Figure 6, it also appears that  $D_{11}$  approaches the equilibrium value  $D_{\text{eq}}$  (indicated by the dashed line) with increasing time.

Values of thermal diffusivity in the flow direction  $D_{11}$  (obtained as shown in Figure 6) and the neutral direction  $D_{33}$  (obtained in the same manner) are shown in Figure 7 as functions of time following the imposition of the step strain for two different values of strain  $\gamma = 4$  and 8. In the flow direc-

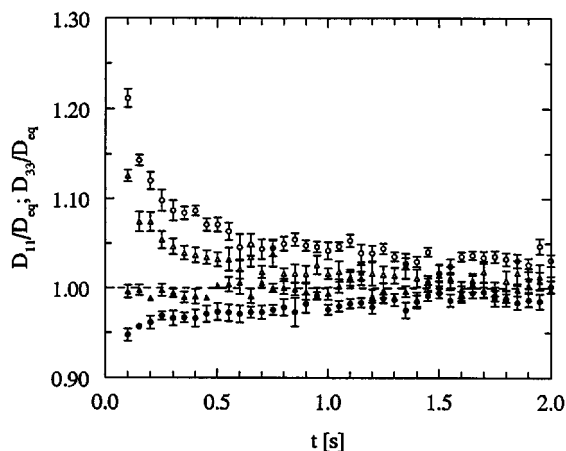


Figure 7. Thermal diffusivity in flow  $D_{11}$  ( $\circ$  strain of eight,  $\triangle$  strain of four) and neutral  $D_{33}$  (filled symbols) directions vs. time following the imposition of a step shear strain of eight.

Error bars for  $D_{11}$  and  $D_{33}$  are estimated from the uncertainty in determining slopes of  $1/\tau_g$  vs.  $4\pi^2/\Lambda^2$ , as shown in Figure 6. The dashed line represents the equilibrium thermal diffusivity measured for a quiescent liquid.

tion, the thermal diffusivity at the largest strain is increased above the equilibrium value by approximately 20% immediately following the step strain. A decrease of approximately five percent is observed in thermal diffusivity measured in the neutral direction. In both cases, the thermal diffusivity appears to be relaxing back to its equilibrium value  $D_{eq}$  (indicated by dashed line). These results confirm the existence of anisotropic thermal diffusivity in polymer melts induced by deformation.

The observation that thermal conductivity, and, hence, thermal diffusivity, is increased in the flow direction suggests that conduction along polymer chain segments is facilitated compared to conduction between different chain segments,

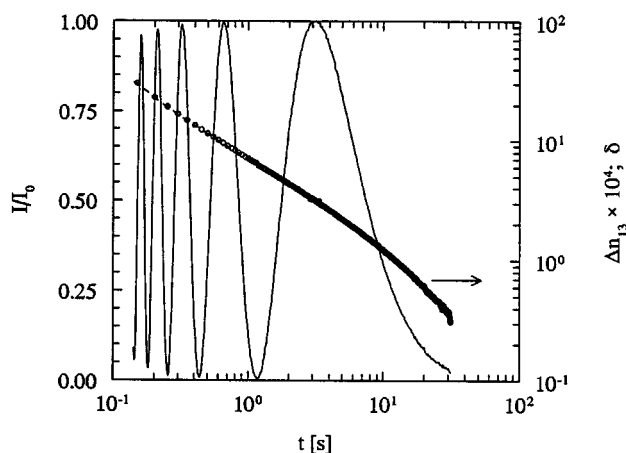


Figure 8. Normalized intensity as a function of time for the birefringence experiment at a strain of eight.

Also shown is the birefringence calculated from the intensity (see Figure 9 for details).

consistent with earlier hypotheses (see van den Brule (1989); van den Brule and O'Brien (1990), and references therein). The results in Figure 7 also suggest that the orientation of chain segments is reduced in the neutral direction following the deformation. Relaxation of the chain segment orientation to an isotropic state would, of course, correspond to the relaxation of the thermal diffusivity to its equilibrium value.

In order to examine the connection between flow-induced chain-segment orientation and anisotropic thermal diffusivity, we also measured the flow-induced birefringence of the polymer melt following the imposition of a step shear strain. It is generally accepted that the refractive index tensor  $\mathbf{n}$  is proportional to the second moment of the chain segment orientation vector  $\mathbf{Q}$  (Fuller, 1995; p. 115)

$$\mathbf{n} = \frac{2\pi\nu}{15} \frac{(\bar{n}^2 + 1)^2}{\bar{n}} \frac{\alpha_1 - \alpha_2}{N_K a_K^2} \langle \mathbf{Q}\mathbf{Q} \rangle, \quad (10)$$

where  $\nu$  is the number density of induced dipole moments in the chain,  $N_K$  is the number of Kuhn steps in the chain segment,  $a_K$  is the length of a Kuhn step,  $\bar{n}$  is the average refractive index for the segment,  $\alpha_1$  is the polarizability along the chain, and  $\alpha_2$  is perpendicular to the chain. This expression is valid if the chains are not stretched too greatly by the flow.

Therefore, non-zero birefringence indicates an anisotropic orientation of chain segments (Janeschitz-Kriegl, 1983). The normalized transmitted intensity is shown in Figure 8 as a function of time, and indicates that the retardance  $\delta$  goes through multiple orders. Using Eqs. 8 and 9 and the data in Figure 8, we plot the relaxation of the birefringence  $\Delta n_{13}$  following the step strain in Figure 9. The birefringence appears to relax on a time-scale comparable to the relaxation of  $D_{11}$  and  $D_{33}$ .

In Figure 10, we plot the thermal diffusivity difference  $D_{11} - D_{33}$  normalized by  $D_{eq}$  vs. the birefringence  $\Delta n_{13}$  such that time following the step strain becomes a parameter. Within experimental uncertainty,  $D_{11} - D_{33}$  is proportional to  $\Delta n_{13}$

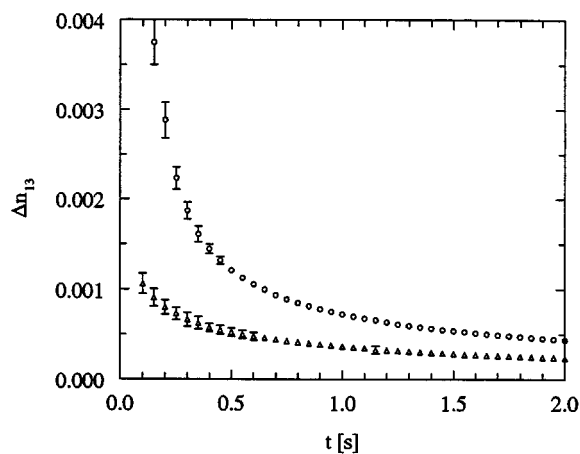


Figure 9. Decay in birefringence  $\Delta n_{13}$  as a convolution of the raw data such as shown in Figure 8, using Eqs. 8 and 9. Symbols defined in Figure 7.

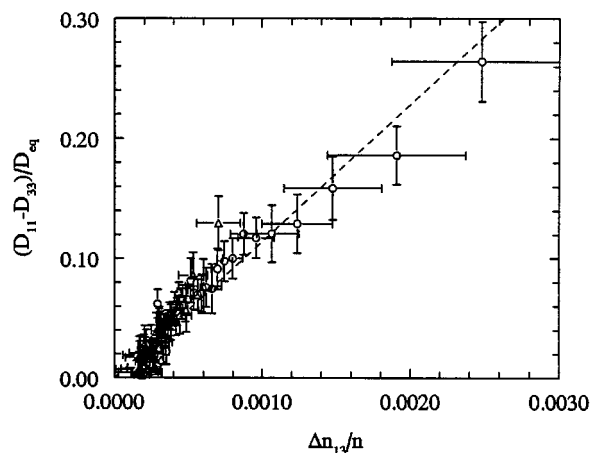


Figure 10. Normalized difference in the thermal diffusivity vs. normalized birefringence for a step shear strains of four and eight.

The solid line through the data ( $\circ$  and  $\triangle$  as in Figure 7) suggests a proportionality between these quantities. Vertical and horizontal error bars were determined as described in caption to Figure 7. The dashed line is the best estimate for the optic-thermal coefficient  $C_1/C$ .

supporting the claim that flow-induced orientation of polymer chain segments is responsible for anisotropy in both optical and thermal transport properties. In addition, the linear relation suggests that the thermal diffusivity also depends upon the second moment of the chain segment orientations. The data shown in Figure 10 when considered in conjunction with the well-established stress-optic rule (Eq. 3) (Janeschitz-Kriegl, 1983), which says the refractive index and stress tensors are proportional, support the validity of a stress-thermal law written as

$$\frac{1}{D_{eq}} \left( D - \frac{1}{3} \delta tr D \right) = C_t \tau, \quad (11)$$

where  $C_t$  is the stress-thermal coefficient.

The stress difference needed to evaluate Eq. 11 is  $N_3 = \tau_{11} - \tau_{33}$ . However, the mechanical measurement of transient normal stresses in undiluted polymer melts is difficult because of transducer compliance effects (Hansen and Nazem, 1975). On the other hand, using a typical value (Janeschitz-Kriegl, 1983) for the stress-optic coefficient of  $2 \times 10^{-10} \text{ dyne}^{-1}$ , we estimate a value for the stress-thermal coefficient  $C_t \approx 10^{-6} \text{ cm}^2/\text{s}$  for the system under consideration. Theoretical developments for flowing polymer systems based on network theories for polymer melts (van den Brule, 1989) suggest that the expression in Eq. 11 is valid. The experimental results reported here support the existence of a stress-thermal law.

In future work, we shall attempt to determine the  $D_{12}$  and  $D_{22}$  components of the thermal diffusivity tensor following step strain deformations. These measurements should be possible with the FRLS technique by choosing appropriate orientations of the grating with respect to the flow. The existence of a stress-thermal law would be of great use in nonisothermal, non-Newtonian fluid mechanics calculations.

## Acknowledgments

The authors are grateful to the National Science Foundation for support of this study through Grant CTS-9509754 and to the Amoco Foundation for matching funds used towards the optical setup.

## Literature Cited

- Bird, R. B., C. F. Curtiss, and K. J. Beers, "Polymer Contribution to the Thermal Conductivity and Viscosity in a Dilute Solution (Fraenkel Dumbbell Model)," *Rheol. Acta*, **36**, 269 (1997).
- Bird, R. B., O. Hassager, R. C. Armstrong, and C. F. Curtiss, *Dynamics of Polymeric Liquids Vol. I: Rheology*, 2nd ed., Addison-Wesley (1987).
- Broerman, A. W., D. C. Venerus, and J. D. Schieber, "Evidence of a Stress-Thermal Rule in an Elastomer Subjected to Simple Elongation," *J. Chem. Phys.*, **111**, 6965 (1999).
- Chitrangrad, B., and J. J. C. Picot, "Similarity in Orientation Effects on Thermal Conductivity and Flow Birefringence for Polymers-Polydimethylsiloxane," *Poly. Eng. Sci.*, **21**, 782 (1981).
- Curtiss, C. F., and R. B. Bird, "Statistical Mechanics of Transport Phenomena: Polymeric Liquid Mixtures," *Adv. Poly. Sci.*, **125**, 1 (1996).
- Eichler, H. J., P. Günter, and D. W. Pohl, *Laser-Induced Dynamic Gratings*, Springer, Berlin (1986).
- Fuller, G. G., *Optical Rheometry of Complex Fluids, Topics in Chemical Engineering*, Oxford University Press, New York and Oxford (1995).
- Hansen, M. G., and F. Nazem, "Transient Normal Force Transducer Response in a Modified Weissenberg Rheogoniometer," *Trans. Soc. Rheol.*, **19**, 21 (1975).
- Janeschitz-Kriegl, H., *Polymer Melt Rheology and Flow Birefringence*, Springer-Verlag, Berlin (1983).
- Köhler, W., C. Rosenauer, and P. Rossmanith, "Holographic Grating Study of Mass and Thermal Diffusion of Polystyrene/Toluene Solutions," *Int. J. Thermophys.*, **16**, 11 (1995).
- Miyamoto, H., and A. Nagashima, "Measurement of Transient Behavior of the Thermal Diffusivity of Flowing Polymer Melt," *Int. J. Thermophys.*, **17**, 1113 (1996).
- Öttinger, H. C., "Relativistic and Nonrelativistic Description of Fluids with Anisotropic Heat Conduction," *Physica A*, **254**, 433 (1998).
- Öttinger, H. C., and F. Petrillo, "Kinetic Theory and Transport Phenomena for a Dumbbell Model under Nonisothermal Conditions," *J. Rheol.*, **40**, 857 (1996).
- Picot, J. J. C., G. I. Goobie, and G. S. Mawhinney, "Shear-Induced Anisotropy in Thermal Conductivity in Polyethylene Melts," *Poly. Eng. Sci.*, **25**, 154 (1982).
- Press, W. H., S. A. Teukolsky, W. T. Vetterling, and B. P. Flannery, *Numerical Recipes in FORTRAN: The Art of Scientific Computing*, 2nd ed., Cambridge Univ. Press, Cambridge, U.K. (1992).
- Rondelez, F., W. Urbach, and H. Hervet, "Origin of Thermal Conductivity Anisotropy in Liquid Crystalline Phases," *Phys. Rev. Letters*, **41**, 1058 (1978).
- Tautz, H., "Bestimmung der Wärmeleitfähigkeit von Kautschukvulkanisaten in Abhängigkeit von der Dehnung," *Exp. Tech. der Phys.*, **7**, 1 (1959).
- van den Brule, B. H. A. A., "A Network Theory for the Thermal Conductivity of an Amorphous Polymeric Material," *Rheol. Acta*, **28**, 257 (1989).
- van den Brule, B. H. A. A., and S. B. G. O'Brien, "Anisotropic Conduction of Heat in a Flowing Polymeric Material," *Rheol. Acta*, **29**, 580 (1990).
- Veletska, D., I. Kapturauskas, and R. Baltrameyunas, "Light-Induced Thermal Grids and the Thermo-optical Effect in Mesophase Liquid Crystals," *Sov. Phys. Tech. Phys.*, **27**, 263 (1982).
- Venerus, D. C., J. D. Schieber, H. Iddir, J. D. Guzmán, and A. W. Broerman, "Measurement of Thermal Diffusivity in Polymer Melts using Forced Rayleigh Light Scattering," *J. Poly. Sci., Polym. Phys. Ed.*, **37**, 1069 (1999).
- Wallace, D. J., C. Moreland, and J. J. C. Picot, "Shear Dependence of Thermal Conductivity in Polyethylene Melts," *Poly. Eng. Sci.*, **25**, 70 (1985).

Manuscript received May 6, 1999, and revision received Nov. 11, 1999.